26th International Conference
ENGINEERING MECHANICS 2020
Brno, Czech Republic, November 24 – 25, 2020

COMPUTATIONAL MODELING OF BLOOD FLOW IN THE BIFURCATION OF HUMAN CAROTID ARTERY

Švancara P.*, Lisický O., Jagoš J.***, Burša J.******

Abstract: *Computational simulations can be used to better predict the risk of atherosclerotic plaques (atheromas) formation. The study presents three-dimensional patient specific computational models of blood hemodynamic in the human carotid arteries based on finite volume method. The geometry of the arteries was created from computer tomography (CT) images. Measured mass flow rate waveform at the inlet and two-element Windkessel model at the outlets are used as boundary conditions. Blood is considered as a non-Newtonian fluid described by Carreau model and pulsating blood flow is solved by transient analysis. Time history of wall shear stress magnitude, velocity profiles in individual cross-sections and flow pattern are evaluated and discussed as they may be helpful in assessing the risk of potential development of atheroma.*

Keywords: Carotid artery, Blood, Windkessel model, Wall shear stress, Computational fluid dynamics.

1. Introduction

Atherosclerosis is responsible for nearly a third of global deaths worldwide. (Caro et al., 1971) suggested flow disturbances and low wall shear stress (WSS) as significant factors in the formation of an atherosclerotic plaque. This hypothesis was then validated by multiple studies summarized in (Malek et al., 1999). One of the approaches to investigate WSS is employing the computational fluid dynamic (CFD) simulation of the blood flow in patient specific models (Cebral et al., 2002; Gharahi et al., 2016). Problem of such simulations is to obtain accurate geometry models, determination of realistic boundary conditions, appropriate viscosity model and inclusion of the wall elasticity.

2. Methods

Geometries of the left and right carotid artery (CA) of 63 year old female patient was semi-automatically reconstructed from CT images in the RETOMO software (BETA CAE Systems); they are shown in Figs. 1a and 1c. The patient already had atheromas formed in both CAs, which were removed manually from the model so that the geometry corresponded to healthy carotid arteries. The finite volume mesh consisting of hexahedral elements was then created in software ANSYS ICEM-CFD, see Figs. 1b and 1d. To test the effect of mesh element size, three meshes with 24 809, 49 289 and 158 576 elements were created for the right CA. Fig. 2b shows an example of computed velocity profiles near the common carotid artery (CCA) inlet at systolic pressure. From the results we can see that velocity profiles differ from each other in the order of percentage units; for further simulations a mesh with 49 289 elements was used. The same element size was used for the left CA. A finite volume method was used to solve fluid dynamic problem using software ANSYS Fluent.

* Ing. Pavel Švancara, PhD.: Institute of Solid Mechanics, Mechatronics and Biomechanics, Brno University of Technology, Technická 2896/2; 616 69, Brno; CZ, svancara@fme.vutbr.cz

** Ing. Ondřej Lisický: Institute of Solid Mechanics, Mechatronics and Biomechanics, Brno University of Technology, Technická 2896/2; 616 69, Brno; CZ, 161238@vutbr.cz

*** Ing. Jiří Jagoš: Institute of Solid Mechanics, Mechatronics and Biomechanics, Brno University of Technology, Technická 2896/2; 616 69, Brno; CZ, 145427@vutbr.cz

**** Prof. Ing. Jiří Burša, PhD.: Institute of Solid Mechanics, Mechatronics and Biomechanics, Brno University of Technology, Technická 2896/2; 616 69, Brno; CZ, bursa@fme.vutbr.cz

doi: 10.21495/5896-3-480

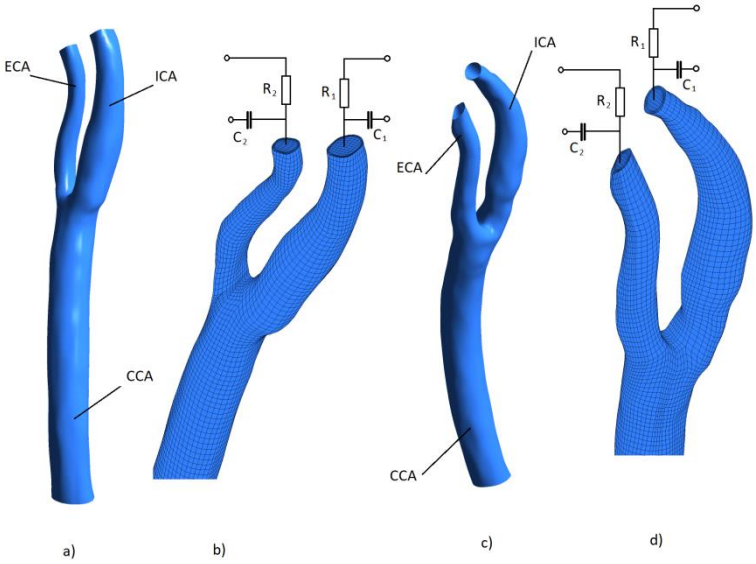

Fig. 1: a) Reconstructed geometry of the left CA; b) Detail of the finite volume mesh of the left CA with scheme of two-element Windkessel model at outlets; c) Reconstructed geometry of the right CA; d) Detail of the finite volume mesh of the right CA with two-element Windkessel model at outlets.

The waveform of mass flow rate obtained from cine phase-contrast MR flow velocity measurements (Cebral et al., 2002) was imposed at the inlet of CCA), see Fig. 2a. The downstream vascular bed was modelled with two-element Windkessel model (Shi et al., 2011) implemented in ANSYS Fluent by ANSYS customization tool Windkessel. The parameters of the outflow network were first estimated according to the pulse pressure method (Stergiopulos et al., 1999) and then iteratively tuned to achieve agreement with the waveforms of mass flow rates in internal carotid artery (ICA) and external carotid artery (ECA) published in literature (Cebral et al., 2002). Parameters used for simulations are summarized in Tab. 1.

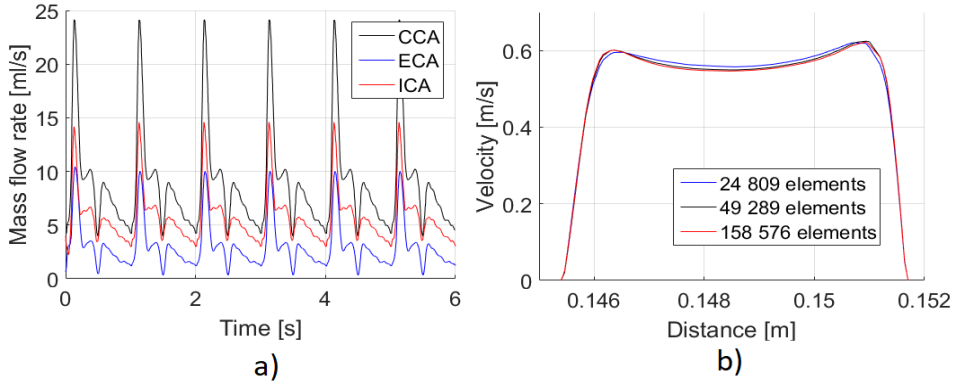

Fig. 2: a) Mass flow rate waveform used as boundary condition at CCA inlet (black) and computed mass flow rates at ECA outlet (blue) and at ICA outlet (red); b) Computed velocity profiles near left CCA inlet for different element sizes (at systolic pressure).

The blood was modelled as non-Newtonian fluid using the Carreau model for which viscosity μ_{eff} depends upon shear rate $\dot{\gamma}$ by the following equation:

$$\mu_{eff}(\dot{\gamma}) = \mu_{\inf} + (\mu_0 - \mu_{inf})\left(1+(\lambda\dot{\gamma})^2\right)^{\frac{n-1}{2}} \quad (1)$$

Where μ_0 is viscosity at zero share rate, $\mu_{\inf}$ is viscosity at infinite shear rate, λ is relaxation time and n is power index. For the present simulations the parameters $\mu_{\inf}$ = 0.0345 Pa.s, μ_0 = 0.56 Pa.s, λ=3.313 s and n = 0.3568 were used (Johnston et al., 2004). Blood flow through CA was computed by a transient analysis with a time step $\Delta t = 2\text{x}10^{-3}$ s and six periods of the cardiac cycle were solved to obtain sustained values.

Tab. 1: Parameters of two-element Windkessel models.

R_1 (ICA)	2.023e9 [kg/m^{4}s]
C_1 (ICA)	7.505e-11 [m^{4}s^2/kg]
R_2 (ECA)	3.811e9 [kg/m^{4}s]
C_2 (ECA)	8.0e-11 [m^{4}s^2/kg]

3. Results a discussion

Fig. 3a shows an example of computed streamlines with colour marked velocity magnitude for the left CA at diastolic pressure for the last solved period of the cardiac cycle. Corresponding velocity profiles in individual cross-sections near bifurcation are shown in Fig. 3b. The same results for the right CA are shown in Figs. 3c and 3d. Computed WSS magnitude distributions at diastolic pressure in global range and range up to 0.4 Pa are shown in Figs. 4a - 4c.

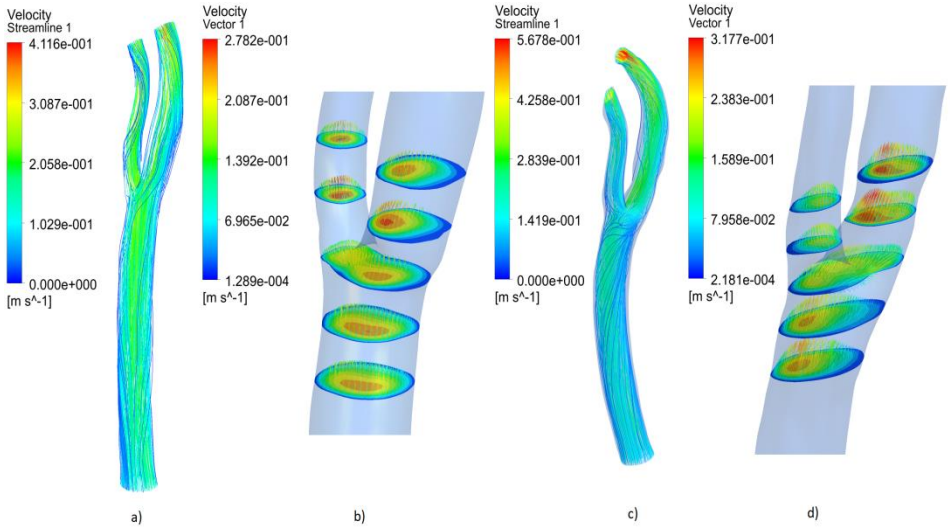

Fig. 3: Flow visualization (diastolic pressure): a) Streamlines with colour marked velocity magnitude for the left CA; b) Velocity profiles in individual cross-sections for the left CA; c) Streamlines for the right CA; d) Velocity profiles for the right CA.

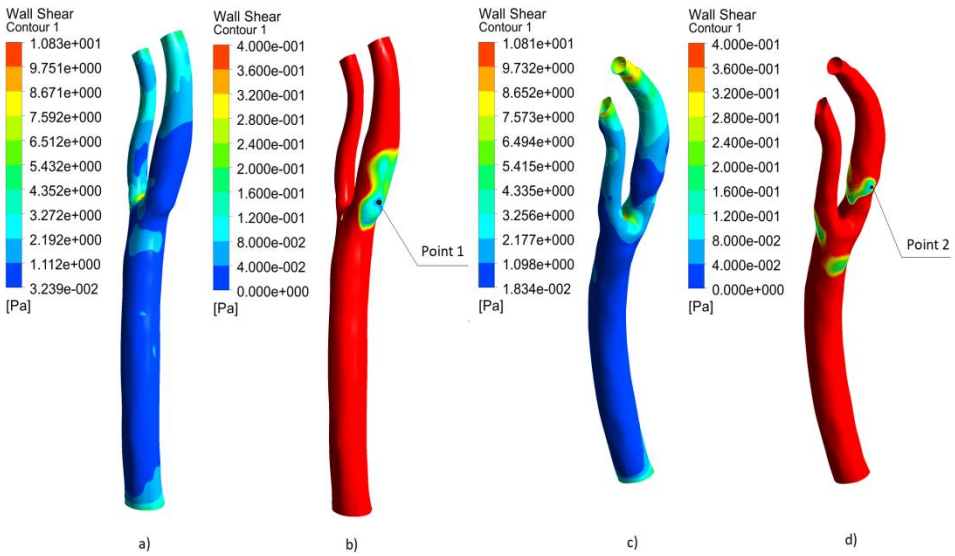

Fig. 4: Visualization of the WSS magnitude distribution (diastolic pressure): a) Left CA in global range; b) Left CA in range up to 0.4 Pa; c) Right CA in global range; d) Right CA in range up to 0.4 Pa.

The results show that on the walls of the analyzed arteries there are areas where the WSS magnitude is less than 0.4 Pa, which is low non-physiologic shear stress that could lead to development of atherosclerotic lesions (Zarins et al., 1983, Malek et al., 1999). These areas are associated with oscillatory and disturbed flow that leads to unsteady distributed flow profile. For left CA the area with low WSS magnitude (< 0.4 Pa) corresponds to the place where the atheroma began to form. For the right CA the atheroma began to form at the site of the bifurcation, which is an area surrounded by places with low WSS. Fig. 5 shows the computed time courses of the WSS magnitude at points 1 and 2 marked in Fig. 4. As we can see, the magnitude of WSS remains bellow 0.4 Pa for a significant time of the cardiac cycle. The authors are aware that the growth of the atheroma may have changed the shape of the CA and the reconstructed geometry may not fully correspond to the state before the atheroma development.

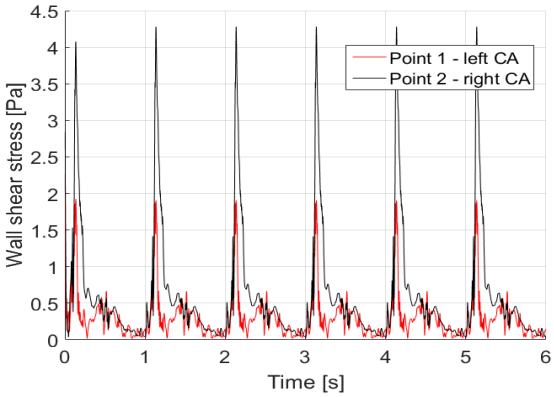

Fig. 5: Computed WSS magnitude at points 1 (left CA) and 2 (right CA).

4. Conclusions

Three-dimensional patient specific computational models of blood hemodynamic in the human carotid arteries were created. Computed results are in good agreement with physiological data published in the literature and the model is capable to predict correctly WSS magnitude, velocity profiles and flow pattern. Locations of low WSS magnitude (< 0.4 Pa) correspond well to locations where the atheroma began to form. Although the process of atheroma formation is generally more complicated and need future research, the developed model may be helpful in guiding future therapeutic strategies.

Acknowledgement

This work was supported by Czech Science Foundation project No. GA18-13663S.

References

Caro, C. G., Fitz-Gerald, J.M., Schroter, R. C. (1971) Atheroma and arterial wall shear-Observation, correlation and proposal of a shear dependent mass transfer mechanism for atherogenesis. Proceedings of the Royal Society of London. Series B. Biological Sciences, 177, 1046, pp. 109-133.

Cebral, J. R., Yim, P. J., Lohner, R. (2002) Blood flow modeling in carotid arteries with computational fluid dynamics and MR imaging. Academic Radiology, 9, 11, pp. 1286-1299.

Gharahi, H., Zambrano, B. A., Zhu, D. et al. (2016) Computational fluid dynamic simulation of human carotid artery bifurcation based on anatomy and volumetric blood flow rate measured with magnetic resonance imaging. Int J Adv Eng Sci Appl Math, 8, 1, pp. 46-60.

Johnston, B. M., Johnston, P. R., Corney, S. et al. (2004) Non-Newtonian blood flow in human right coronary arteries: steady state simulations. Journal of Biomechanics, 37, 5, pp. 709-720.

Malek, A. M., Alper, S. L., Izumo, S. (1999) Hemodynamic shear stress and its role in atherosclerosis. Jama, 282, 21, pp. 2035-2042.

Shi, Y., Lawford, P., Hose, R. (2011) Review of zero-D and 1-D models of blood flow in the cardiovascular system. Biomed Eng OnLine, 10, 33.

Stergiopulos, N., Segers P., Westerhof, N. (1999) Use of pulse pressure method for estimating total arterial compliance in vivo. Am. J. Physiol. - Hear. Circ. Physiol., 276, 2, pp. 424-428.

Zarins, C. K., Giddens, D. P., Bharadvaj, B. K. et al. (1983) Carotid bifurcation atherosclerosis. Quantitative correlation of plaque localization with flow velocity profiles and wall shear stress. Circulation research, 53, 4, pp. 502-514.